DOI: https://doi.org/10.52651/sam.a.2021.1.14-18

DILATOMETRIC ANALYSIS TOOL STEEL X153CRMOV12

Michal KRBAŤA, Róbert CÍGER

Abstract: The article deals with phase transformations and austenitizing behavior of the X155CrMoV12 tool steel. Dilatation analyses of a series of samples were performed at various cooling rates, chosen in the range from 10 °C·s^{-1} to 0.1 °C·s^{-1}. Acquired experimental data were used for evaluation of dilatometric curves in order to map the temperature ranges of phase transformations of the austenite to pearlite, bainite or martensite. All experimental samples from dilatometric analyses were then subjected to microstructural analyses and hardness measurements to characterize the microstructure and hardness for every tested heat treatment regime. The second part of this article, entitled "EXPERIMENTAL DETERMINATION OF CONTINUOUS COOLING TRANSFORMATION DIAGRAM FOR HIGH STRENGTH STEEL X153CRMOV12", deals with these analyses of the cooling curve microstructure.

Keywords: ARA diagram; Tool steel; Dilatometry; Compression test.

1 INTRODUCTION

Some currently produced steels with extreme high content of carbide forming elements are known as ledeburitic steels. Ledeburitic structure is typical for white cast irons with carbon content above 2.11 wt. % as is shown in the Fe-Fe_3C metastable binary diagram in Fig. 1 [1, 2]. However, alloying element present in the ledeburitic steel extend the area of the ferrite and narrow area of the austenite. Consequently, the eutectoid point S and the point of maximum solubility of carbon in austenite – E are moved to the lower carbon content values. Due to this effect, ledeburite is present in structure of these steels at carbon content below 2.11 wt. %. Common carbon content in ledeburitic steels is higher than 0.7 wt. %. At lover carbon content, there would be present a certain amount of δ-ferrite, negatively influencing the hardness [3].

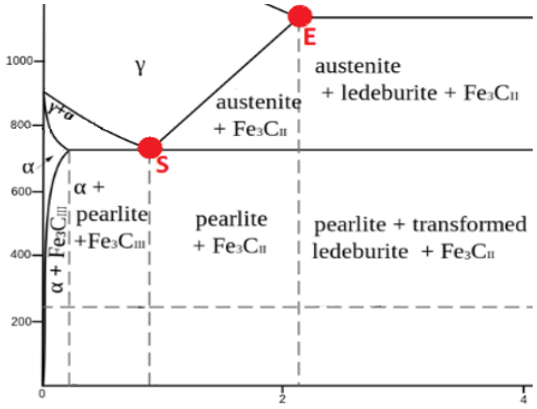

Fig. 1 Selected part of phase diagram Fe-Fe_3C binary system
Source: authors.

2 MATERIALS AND METHODS

The experimental material used in these experiments is high-alloy tool steel X153CrMoV12 used in the engineering industry. It is a high hardenability chromium-vanadium steel suitable for oil and air hardening [4]. Steel is characterized by high wear resistance and is mostly used for cutting tools such as tensioning and extrusion mandrels, profile sheets and complex shaped cutters. The chemical composition of the experimental samples was verified with a TASMAN Q4 spectrum analyser and is listed in Tab. 1. Its basic mechanical and physical properties are listed in Tab. 2.

Tab. 1 Chemical composition of steel X153CrMoV12 (wt.%)

Element	Min - Max	Spectral analysis
C	1.45-1.60	1.53 ± 0.01
Mn	0.20-0.60	0.21 ± 0.005
Si	0.10-0.40	0.14 ± 0.005
Cr	11.00-13.00	12.25 ± 0.02
Mo	0.70-1.00	0.89 ± 0.01
V	0.70-1.00	0.76 ± 0.01

Source: authors.

Tab. 2 Basic mechanical and physical properties of X153CrMoV12 steel

Mechanical and physical properties	Value
Tensile strength (MPa)	650 - 880
Modulus of elasticity (GPa)	198
Thermal conductivity (W·m^{-1}·K^{-1})	25
Hardness (HV)	790
Specific therm. capacity (J·kg^{-1}·K^{-1})	460

Source: authors.

The base material was supplied in the form of bars with a diameter of 10 mm and a length of 1000 mm. The supplied material is produced in electric furnaces

with the possibility of treatment of liquid steel in secondary metallurgy units. The base material was in a soft annealed state with heating to a temperature just below. Ac1 in the whole cross section, followed by cooling in an oven at a rate of 20 °C/h with a maximum hardness of 270 HV. The microstructure of the base preparation showed a distribution of course and fine spheroidized carbide particles in the ferrite matrix, which is highly machinable and offers less resistance to deformation compared to other microstructures formed during hardening of tool steels.

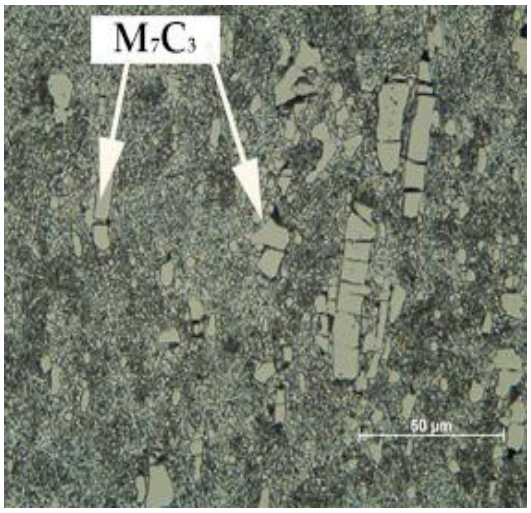

Fig. 2 Basic microstructure of X153CrMoV12 in the normalized state observed-LOM
Source: authors.

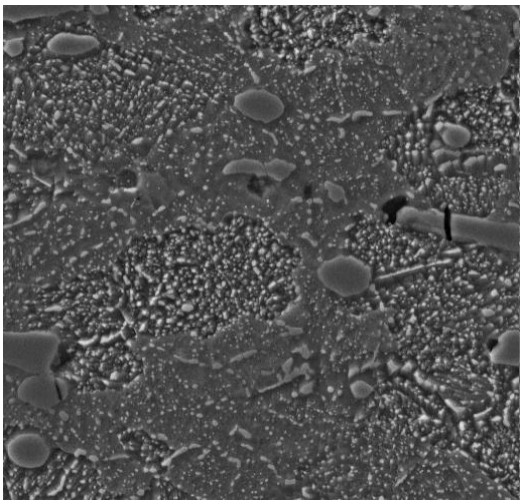

Fig. 3 Basic microstructure of X153CrMoV12 in the normalized state observed-SEM
Source: authors.

The larger particles of distributed spheroidized carbides shown in Fig. 2 and Fig. 3 are primary M_7C_3 carbides that formed during solidification and that dispersed because of heat treatment. Finer carbides ($M_{23}C_6$) originate from secondary precipitation in the spherodization of carbides produced by the transformation of austenite to the microstructure of ferrite carbides by cooling after earlier normalization of the heat treatment (Fig. 4).

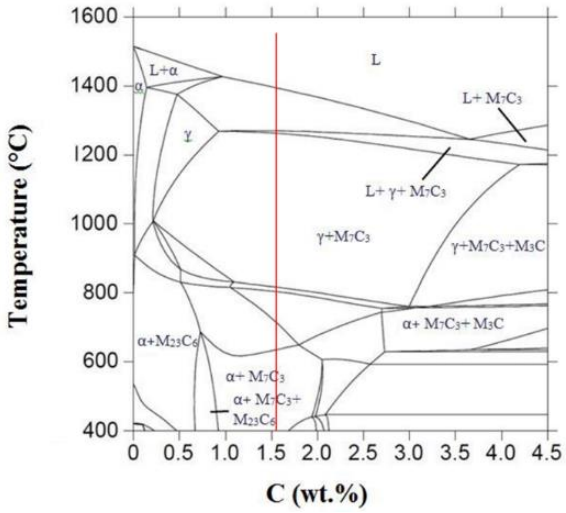

Fig. 4 Calculated phase diagram for X153CrMoV12 steel
Source: authors.

3 RESULT AND DISCUSSION

Phase change occurs in the dilatation curve as a step change in length of the experimental sample. For example, critical temperature Ac_1 corresponds with temperature where the sample starts to contract due to the austenite formation in contrast to the linear expansion during heating. Then, the Ac_3 critical temperature is defined as a temperature where the expansion of the sample starts to be linear again. Heating conditions were the same for all experimental samples, therefore the initial and final austenitizing critical temperatures are constant. Their values for X153CrMoV12 steel are Ac_1=820 °C and Ac_3=850 °C and can be seen in Fig. 5 and Fig. 6.

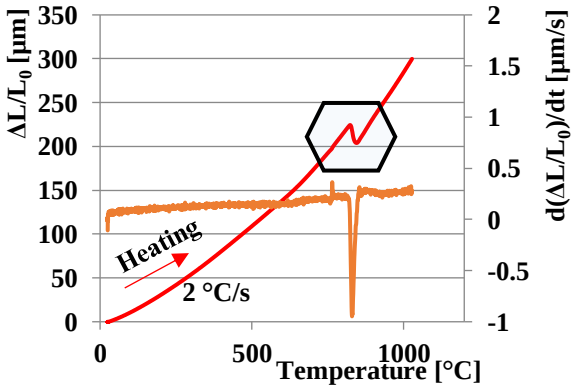

Fig. 5 Determination of transition temperatures Ac_1 and Ac_3 with continuous heating at 2 °C·s^{-1}
Source: authors.

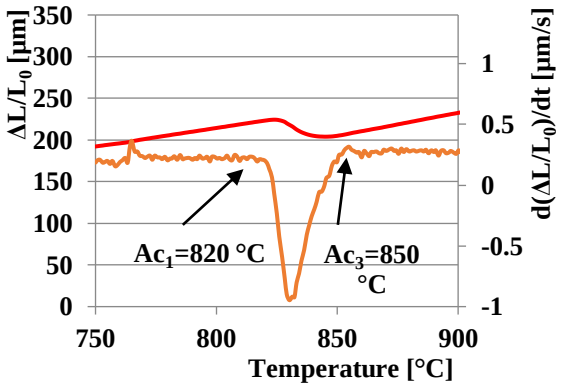

Fig. 6 Increase the area of the expansion curve with Ac_1 and Ac_3
Source: authors.

In Fig. 7, there are visible cooling curve and microstructure of the sample cooled at the rate of 10 °C·s^{-1}. According to dilatometry, Ms temperature was determined as 260 °C (Fig. 7). This temperature represents a rate when only the martensitic matrix and the excluded carbides appear in the structure. The following figure (Fig. 8) the results for sample cooled with rate of 5 °C·s^{-1} are shown. There was observed martensite formation start at 260 °C. In the given curve, the first slight decrease is visible through the derivation, which represents the beginning of the bainite formation immediately followed by the second decrease, which represents the instant formation of the martensite.

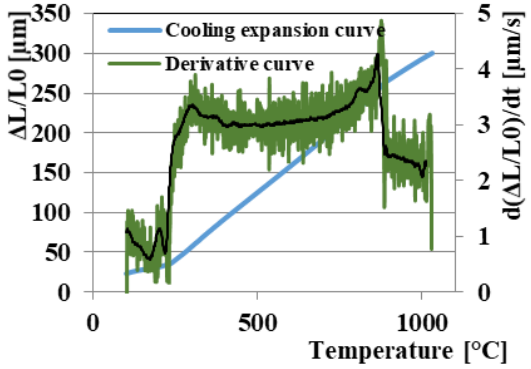

Fig. 7 Analysis of the cooling curve 10 °C·s^{-1}
Source: authors.

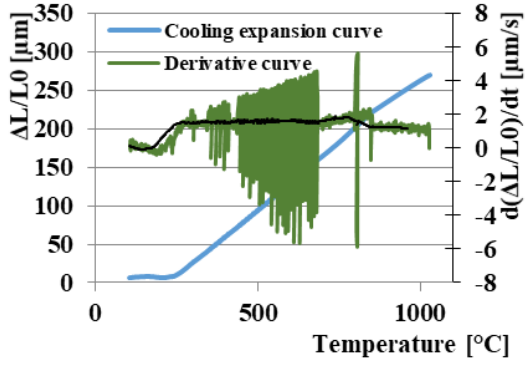

Fig. 8 Analysis of the cooling curve 5 °C·s^{-1}
Source: authors.

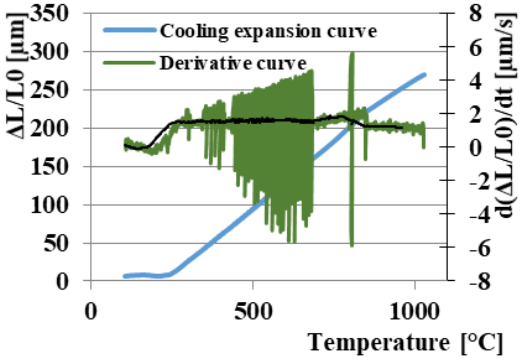

Fig. 9 Analysis of the cooling curve 3 °C·s^{-1}
Source: authors.

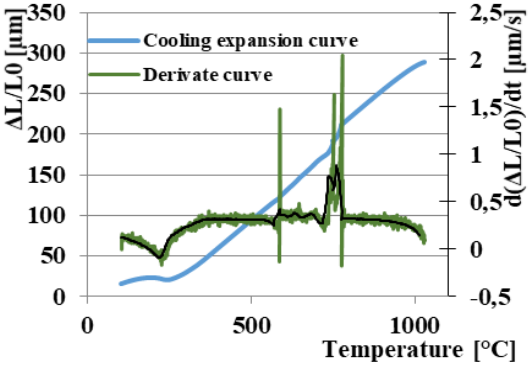

Fig. 10 Analysis of the cooling curve 1 °C·s^{-1}
Source: authors.

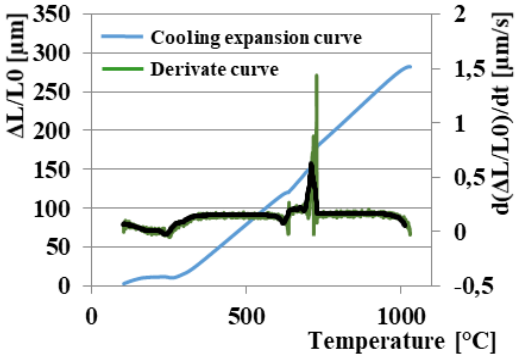

Fig. 11 Analysis of the cooling curve 0.5 °C·s^{-1}
Source: authors.

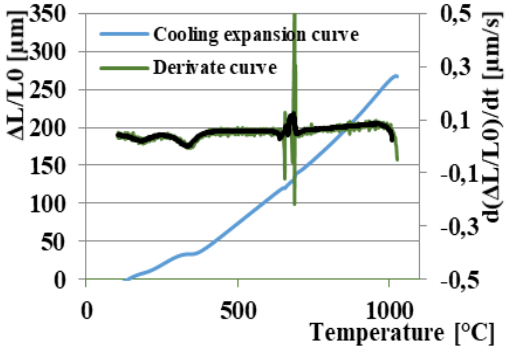

Fig. 12 Analysis of the cooling curve 0.2 °C·s^{-1}
Source: authors.

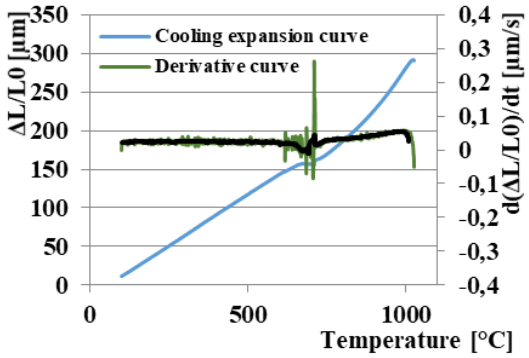

Fig. 13 Analysis of the cooling curve 0.1 °C·s^{-1}
Source: authors.

Further cooling curve (Fig. 9) represents a cooling rate of 3 °C·s^{-1}. In the length change curve, two transitions of transformation are visible. The first one began at 290 °C, which indicates the start of bainite formation and the second at 262 °C, which represents the transformation to martensite. From the derivation of the curve, precipitation of carbides is visible at 585 °C. At a cooling rate of 1 °C·s^{-1}, the bainite formation started at 340 °C. The martensite formation was shifted to 297 °C (Fig. 10). Furthermore, a cooling rate of 0.5 °C·s^{-1} was evaluated (Fig. 11). The beginning of the precipitation of the carbides is visible in the dilatation curve at 689 °C. The bainite formation began at 350 °C and the final transformation to martensite was visible below 250 °C. The next cooling rate was set to 0.2 °C·s^{-1} (Fig. 12). The precipitation of the carbides started at 689 °C. Bainite transformation Bs started at 400 °C and the martensite transformation temperature Ms was 300 °C. The results from the lowest cooling rate (0.1 °C·s^{-1}) are visible in Fig. 13. At the beginning of the cooling, which is the area of the start of the pearlite formation Ps from the austenite. The start of the transformation occurred at 705 °C and its end Pf was at 648 °C. As the dilatation curve continues, a transition through a bainitic transformation begins at a temperature of 430 °C. The transformation to martensite is no longer visible on the dilatometric curve. Therefore, it is possible to predict that the bainitic and martensitic transformation was associated, i.e. the limit value of the transformation to martensite is occurred.

4 CONCLUSION

The phase transformation kinetics under continuous cooling conditions was examined in detail using dilatometry. The higher percentage of chromium in the material results in the formation of Cr_7C_3 carbide, which results in an increased value of the hardness of the material [5, 6]. Provided the martensitic transformation is achieved, the resulting critical cooling rate is set at 5 °C·s^{-1}. This rate, which is precisely bordered by the literature sources, suggests that triple tempering should be followed to achieve the resulting uniform structure of the material. The results of chromium carbides show a fact, that at high cooling rates the incidence of hard carbides is occurred.

References

[1] JURČI, P. *Nástrojové ocele ledeburitického typu (Ledeburitic tool steels).* Praha: CVUT, 2009. p. 221–225. ISBN 978-80-01-04439-1.

[2] YANG, J., B. CAO, Y. WU, Z. GAO and R. HU. Continuous cooling transformation (CCT) behavior of a high Nb-containing TiAl alloy. In: *Acta Materialia*. 2019, **5**(17), p. 1589–1599. ISSN 2589-1529. Available at: https://doi.org/10.1016/j.mtla.2018.11.018

[3] JURČI, P. and L. JANKA. Wear resistance of sub-zero processed Cr-V ledeburitic steel vanadis 6. In: *Metal 2012: 21st International Conference on Metallurgy and Materials*. 2012, p. 635-639. ISBN 978-80-87294-29-1.

[4] BERKOWSKI, L. The influence of warm plastic deformation on the structure and on the applicable properties of highspeed steel. In: *Journal of Materials Processing Technology*. 1996, **60**(1-4), p. 637-641. ISSN 0924-0136. Available at: https://doi.org/10.1016/0924-0136(96)02398-9

[5] ECKERT, M. *Analýza a modelovanie správania sa nástrojových ocelí pri tvárnení za tepla* (Analysis and modeling of hot forming behavior of tool steels). Trenčín: Trenčianska univerzita A. Dubčeka, 2020. p. 90.

[6] ECKERT, M., M. KRBAŤA, I. BARÉNYI, J. MAJERÍK, A. DUBEC and M. BOKES. Effect of selected cooling and deformation parameters on the structure and properties of AISI 4340 steel. In: *Materials*. 2020, **13**(23), p. 5585-5606. ISSN 1996-1944. Availale at: https://doi.org/10.3390/ma13235585

Dipl. Eng. Michal **KRBAŤA**, PhD.
Department of Engineering Technologies and Materials
Faculty of Special Technology
Alexander Dubček University of Trenčín
Ku kyselke 469
911 06 Trenčín
Slovak Republic
E-mail: michal.krbata@tnuni.sk

Dipl. Eng. Róbert **CÍGER**
Department of Engineering Technologies and Materials
Faculty of Special Technology
Alexander Dubček University of Trenčín

Ku kyselke 469
911 06 Trenčín
Slovak Republic
E-mail: robert.ciger@tnuni.sk

Michal Krbaťa – was born in Trenčín, Slovakia in 1988. He received his Master and PhD. degrees at Alexander Dubček University of Trenčín, Faculty of Special Technology in Trenčín. In his research he focuses on materials research, tribology and dilatometry.

Róbert Cíger – was born in Trenčín, Slovakia in 1996. He received his Master degrees at Alexander Dubček University of Trenčín, Faculty of Special Technology in Trenčín. In his research he focuses on materials research, dilatometry.